

Supporting Information for: “*Ab Initio* Investigation of the
Resonance Raman Spectrum of the Hydrated Electron”

Saswata Dasgupta, Bhaskar Rana, and John M. Herbert*

August 21, 2019

*herbert@chemistry.ohio-state.edu

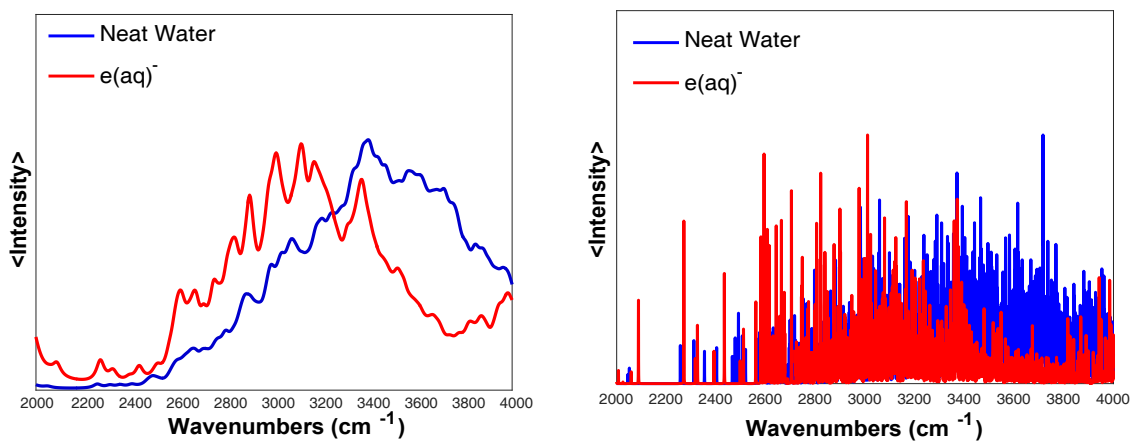


Figure S1: Ensemble-averaged resonance Raman spectrum for $e^-(aq)$ and normal Raman spectrum for neat liquid water, using Lorentzian functions of width (a) 45 cm^{-1} and (b) 0.5 cm^{-1} to broaden the “stick spectra” that are obtained from vibrational frequency calculations on individual structural snapshots. The narrow line width representation in (b) is very close to the stick spectra themselves, with a 0.5 cm^{-1} width added simply for visual clarity. A red shift between the $e^-(aq)$ and the liquid water spectrum is evident even in the dense forest of sticks shown in (b), indicating that this shift is not an artifact of the broadening procedure that is used to obtain a continuous spectral envelope.

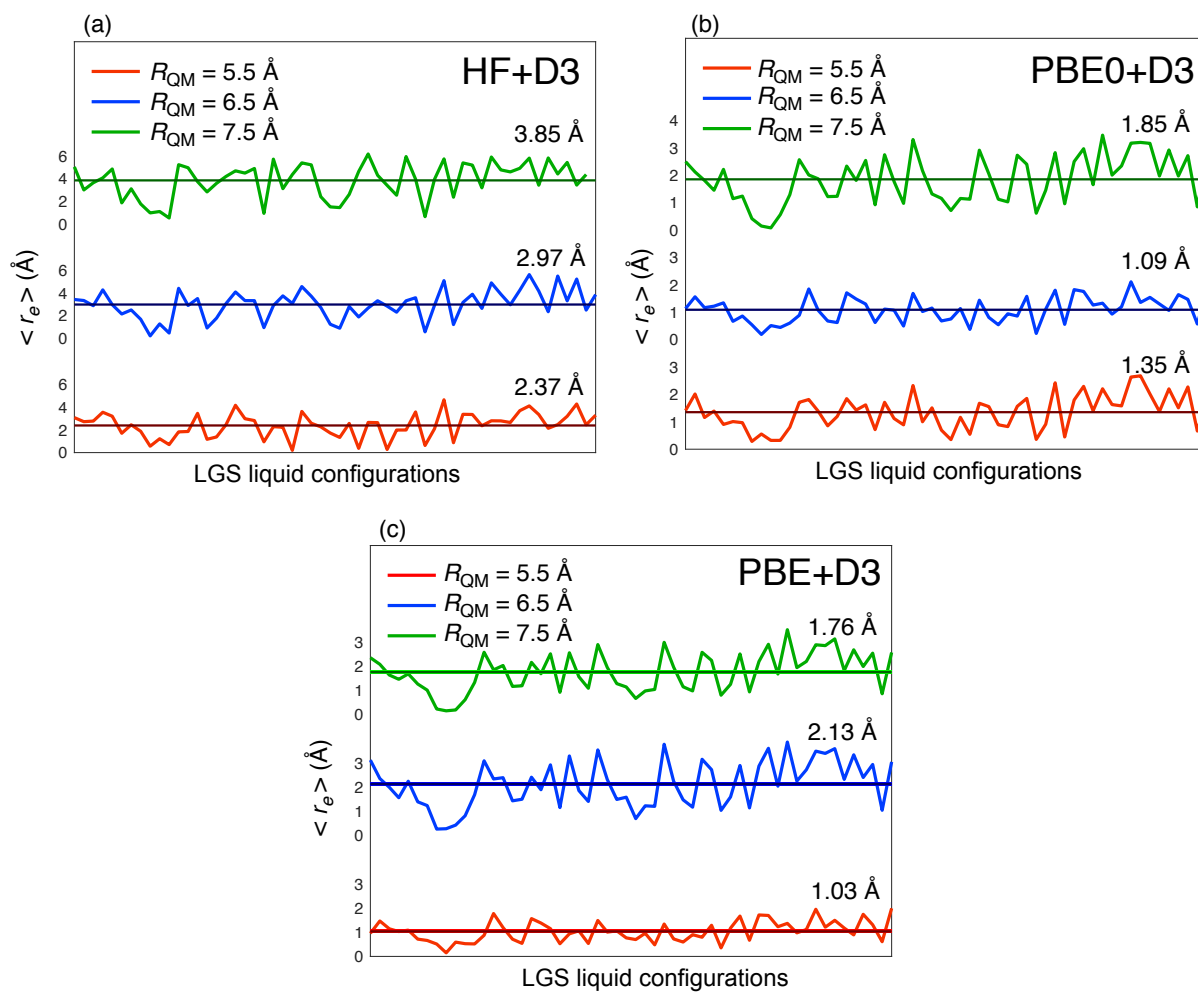


Figure S2: Center of the e^- (aq) spin density for QM/MM calculations at geometries extracted from LGS pseudopotential simulations. This quantity is defined by the expectation value $\langle r_e \rangle$, where r_e is the electron coordinate, with $r_e = 0$ defined by the center of mass of the QM region. The calculations use three different QM radii and are performed at three different levels of SCF theory: (a) HF+D3/6-31+G*, (b) the PBE0+D3/6-31G*, (c) the PBE/3-21++G*. The ensemble-averaged value of $\langle r_e \rangle$ over all snapshots is indicated in each case. The average number of water molecules included in the QM region is 35, 51, and 75 $R_{QM} = 5.5$ Å, 6.5 Å, and 7.5 Å, respectively.

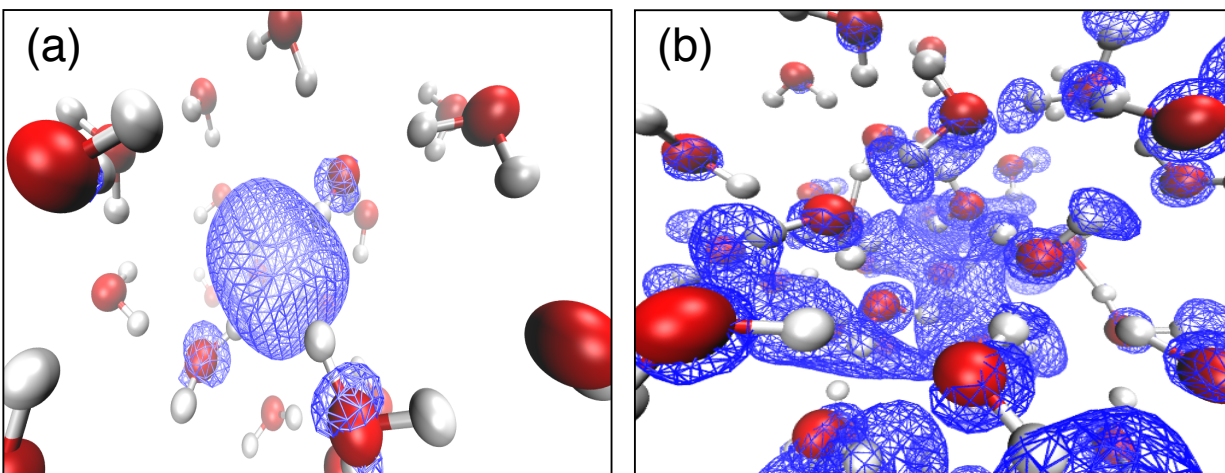


Figure S3: Snapshots the QM region and the spin density of $e^-(aq)$, computed at the HF+D3/3-21++G* level at representative geometries taken from (a) a QM/MM simulation at the HF+D3/3-21++G* level, and (b) a simulation using the LGS pseudopotential. The snapshot in (a) is the same as that shown in Fig. 1 but with the MM water molecules removed for clarity, and this image clearly shows an unpaired electron in a bound state. At the LGS geometry used in (b), however, the SOMO energy level is unbound at the HF+D3/3-21++G* level of theory, leading to a spin density that is delocalized throughout the entire QM region. This represents a greater degree of delocalization that is observed using the LGS pseudopotential itself. This pseudopotential is known to be overly attractive,^{1,2} and the *ab initio* calculation in panel (b) suggests this behavior artificially stabilizes $e^-(aq)$ in liquid geometries where all-electron quantum chemistry finds only unbound continuum states when a negative charge defect is introduced. This result, in conjunction with the fact that the HF+D3 and PBE0+D3 energy level ϵ_{SOMO} is unbound across the entire LGS trajectory, suggest that nothing remotely close to the LGS liquid geometries will stabilize $e^-(aq)$.

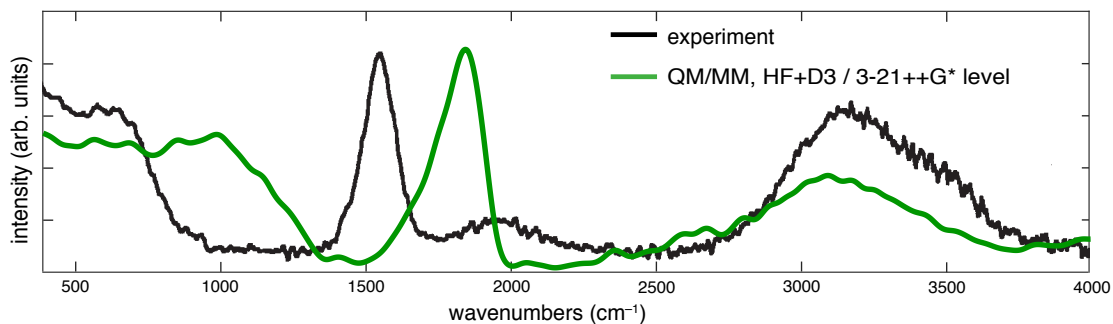


Figure S4: Broad-band, ensemble-averaged resonance Raman spectrum for e^- (aq) computed from a QM/MM simulation at the HF+D3/3-21++G* level and compared to the experimental resonance Raman spectrum from Ref. 3. All qualitative features of the experimental spectrum are reproduced, although the frequency calculations are not quantitative due to neglect of anharmonicity and other limitations of the modeling.

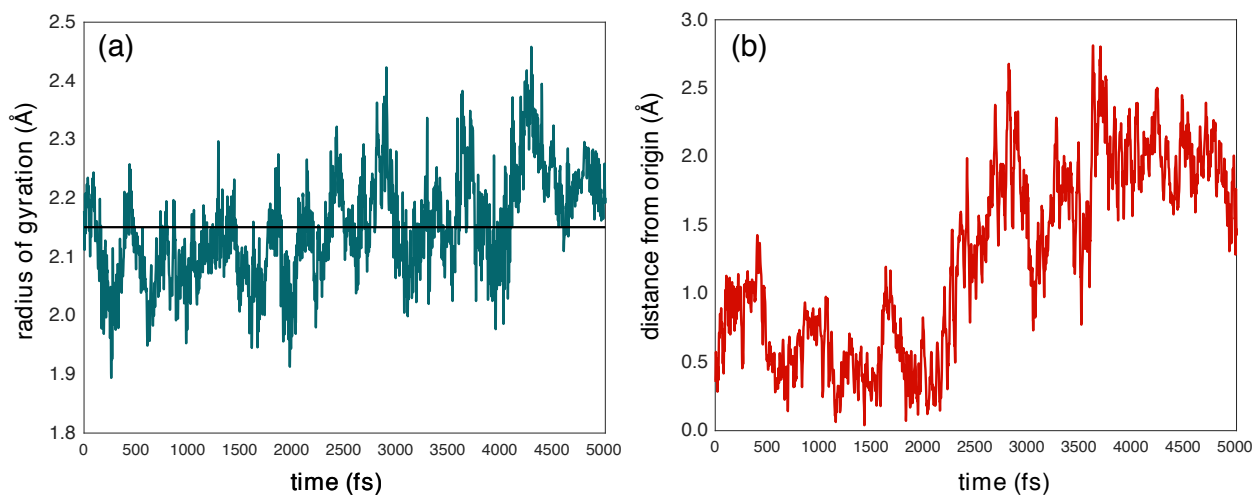


Figure S5: (a) Radius of gyration (r_{gyr}), and (b) distance (r_e) between the centroid of the spin density and the center of mass of the QM region, for a representative QM/MM trajectory at the HF+D3/3-21++G* level. The average value $\langle r_{\text{gyr}} \rangle = 2.15 \text{ \AA}$ is indicated in (a). The radius of the QM region is 5.5 \AA in this simulation, and in (b) we can observe the gradual drift of e^- (aq) towards interface between QM and MM regions, beginning around $t \sim 2 \text{ ps}$.

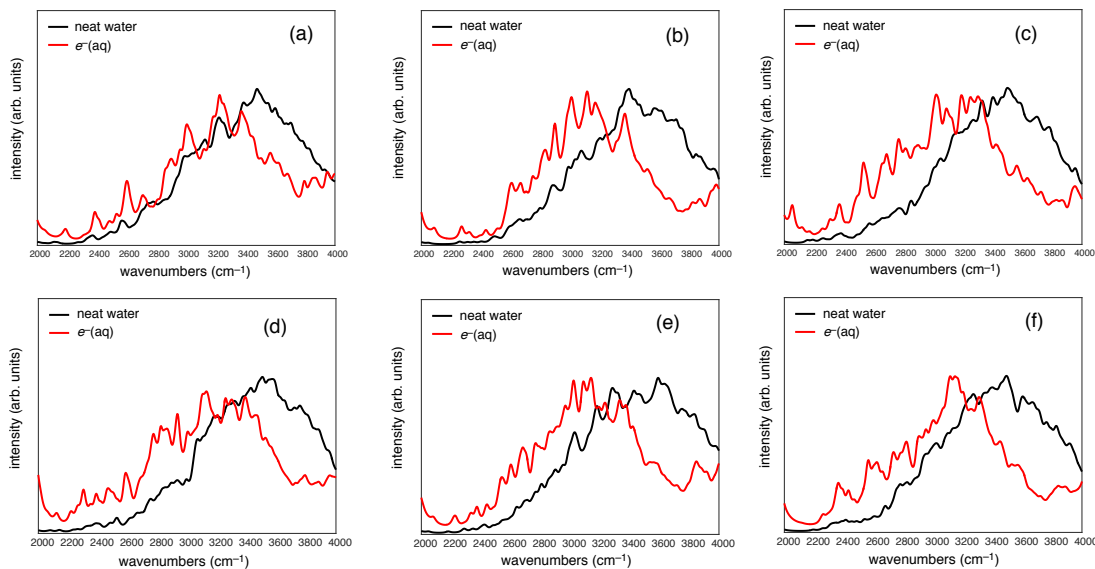


Figure S6: Ensemble-averaged resonance Raman intensities for $e^{-}(\text{aq})$, and normal Raman intensities for neat liquid water, computed at the HF+D3/3-21++G* level of theory using snapshots from six different QM/MM trajectories, each of which is 1 ps in length. A red shift is evident in every case. The average of these six trajectories constitutes the spectrum that is shown in Fig. 7. These data demonstrate that the ensemble average in Fig. 7 is representative of the behavior of each individual trajectory.

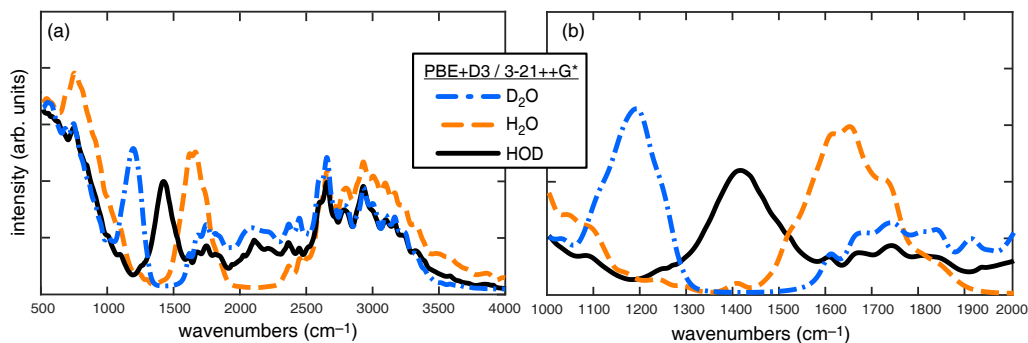


Figure S7: Ensemble-averaged RR intensities for $e^{-}(\text{aq})$ in H_2O , D_2O , and HOD, computed at the PBE/3-21++G* level based on snapshots from LGS pseudopotential simulation. Unlike the analogous bending spectrum obtained from the cavity model, (Fig. 8b), controlled isotopic substitution for HOD does not lead to any splitting of the bending peak for these non-cavity geometries. In addition, the stretching region for HOD is broadened due to the large distribution of electric field strengths experienced by the O–H and O–D oscillators. The “two hump” lineshape in the stretching region that emerges naturally from cavity geometries (Fig. 8a), in agreement with experiment,³ is not observed in these spectra.

References

- [1] Turi, L.; Madarász, A. Comment on “Does the hydrated electron occupy a cavity?”. *Science* **2011**, *331*, 1387.
- [2] Jacobson, L. D.; Herbert, J. M. Comment on “Does the hydrated electron occupy a cavity?”. *Science* **2011**, *331*, 1387.
- [3] Tauber, M. J.; Mathies, R. A. Structure of the aqueous solvated electron from resonance Raman spectroscopy: Lessons from isotopic mixtures. *J. Am. Chem. Soc.* **2003**, *125*, 1394–1402.